J Therm Anal Calorim (2011) 106:347–354
DOI 10.1007/s10973-011-1571-0

Thermal behavior study of biodiesel standard reference materials

Eveline De Robertis · Gabriela F. Moreira · Raigna A. Silva · Carlos A. Achete

CBRATEC7 Conference Special Issue

Abstract Quality control of fuel-related properties of biodiesel, such as thermal stability, is needed to obtain consistent engine performance by fuel users, since biodiesel is susceptible to auto-oxidation when exposed to air, light, and temperature during storage. In this work two pure standard reference materials of biodiesels produced from soy oil and animal feedstocks were studied. Differential scanning calorimetry and thermogravimetry measurements were performed and the analysis of the results revealed small temperature variations in the thermal events among the two standards, these differences are due mainly to their chemical composition, been highly influenced by the amounts of unsaturated esters.

Keywords Standard reference material · Thermal analysis · Biodiesel

Introduction

The increase in petroleum derived products price due to fossil fuels graduate depletion, as well as aspects related to environmental pollution and global warming has caused researchers to seek alternative fuels. Biodiesel has been shown to be a good alternative because it is easy to manufacture on a large scale [1] and provide environmental benefits since it is originated from renewable sources. Studies showed that the incorporation of biodiesel in diesel reduces emissions of CO, CO_2, and sulfur [2, 3].

Biodiesel is chemically defined as composed by mono- or di-alkyl esters of vegetable oils or animal fat, obtained by a reaction known as transesterification, where the triglycerides that constitute the raw materials react with methanol or ethanol in the presence of a strong base (Fig. 1).

Energy sources diversification is important from the standpoint of self-sufficiency, for such biofuels are being introduced aimed at sustainability. The increase in production and consumption of biodiesel involves the development of specific methodologies from production to consumption.

To be commercialized, the biodiesel must possess certain physical and chemical characteristics in accordance with the country laws related to this subject, as for example, their oxidative stability and their flow properties. The oxidative induction time (OIT) is used to estimate the relative stability of samples exposed to an oxidizing atmosphere and therefore determines the substance resistance to oxidation. The conditions are usually those described by the methodology EN 14112. Studies of oxidative stability are very important for quality control of oils and biodiesels regarding their storage [4–9]. The flow properties of biodiesel at low temperatures affect their performance as a fuel in moderate climates, especially during winter. This temperature decrease causes crystallization of the saturated esters present in biodiesel [10, 11]. These crystals can restrict and/or block the fuel flow in the vehicle pipes and filters when it is injected into the engine.

E. De Robertis (✉) · G. F. Moreira · R. A. Silva · C. A. Achete
Divisão de Metrologia de Materiais, Instituto Nacional de Metrologia, Normalização e Qualidade Industrial, Av. Nossa Senhora das Graças, 50, Duque de Caxias, RJ 25250-020, Brazil
e-mail: erobertis@inmetro.gov.br

R. A. Silva
Instituto de Física, Universidade Federal de Uberlândia, Uberlândia, MG, Brazil

C. A. Achete
COPPE, Programa de Engenharia Metalúrgica e de Materiais, UFRJ, Rio de Janeiro, RJ, Brazil

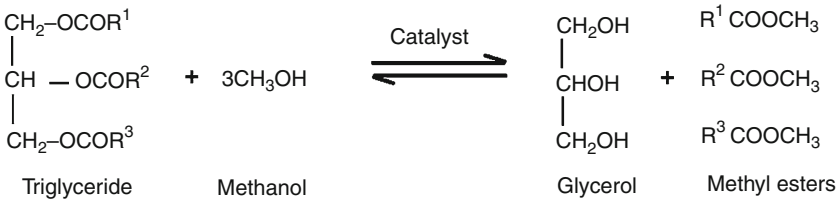

Fig. 1 General equation of transesterification. Adapted from [1]

Recently a review about thermal stability of biodiesels and its blends was published [12], it focused in the importance of the methodologies applied not only to quantify how much the biodiesel was degraded but also to determine which products are formed and the mechanisms involved in such reactions. However, the co-relation between the results from various methods found in the literature is very poor, and much effort must be done in this direction. Besides that the complexity of the substances, which composition is influenced by a large number of factors, adds some complications to the studies.

The application of thermal analysis (TA) techniques such as differential scanning calorimetry (DSC) and thermogravimetric (TG) analysis has become a faster alternative for thermal behavior studies, since by the standard method for such determinations the major drawback is the time of analysis.

In this work, our intention is verify the thermal behavior of two standard reference materials (SRM) using DSC, such technique can provide useful information about crystallization temperature (T_C), melting point (MP), boiling point (BP), and thermal decomposition. By combination DSC results with the analysis obtained with TG coupled to Fourier transform infrared spectrophotometer (FTIR), we can obtain information about degradation and oxidation products depending on the experimental conditions.

Experimental

In this work, two SRM were used; both are 100% (B100) biodiesels produced from soy oil (SRM 2772) and animal feedstocks (SRM 2773). The development of these products is the result of collaboration between National Institute of Standards and Technology (NIST) and National Institute of Metrology, Standardization and Industrial Quality (Inmetro). These materials are certified for physical–chemical properties and some selected reference values are also provided [13, 14].

Table 1 represents biodiesels chemical composition; these biodiesels were obtained by methanol route and therefore, some pure methyl esters present in higher amounts were also investigated. These methyl esters were purchased form Sigma-Aldrich with purity >99%, GC grade: methyl laurate $CH_3(CH_2)_{10}COOCH_3$ (C12:0), methyl myristate $CH_3(CH_2)_{12}COOCH_3$ (C14:0), methyl palmitate $CH_3(CH_2)_{14}COOCH_3$ (C16:0), methyl stearate $CH_3(CH_2)_{16}COOCH_3$ (C18:0), methyl oleate $CH_3(CH_2)_7CH = CH(CH_2)_7COOCH_3$ (C18:1), methyl linoleate $CH_3(CH_2)_3(CH_2CH = CH)_2(CH_2)_7COOCH_3$ (C18:2), and methyl linolenate $CH_3(CH_2)_3(CH_2CH = CH)_3(CH_2)_7COOCH_3$ (C18:3).

DSC experiments were conducted using a DSC Q2000 (TA Instruments) with RCS cooling system. Baseline was calibrated with sapphire disk (supplied by fabricant); cell constant (enthalpy) and temperature were calibrated using indium (NIST SRM #2232) according to standard procedures ASTM E967 and E968.

Two different sets of experiments were made under N_2 dynamic atmosphere (50 mL/min), the first one consisted of cooling the samples (1–3 mg), sealed in an aluminum hermetic pan, in a temperature range from 20 to −90 °C with a rate of 0.5 °C/min. After 2 min at this temperature, the heating curve was obtained by heating the system at the same rate until 20 °C. The second set was conducted in an aluminum pan without lid (open) and higher masses (ca. 10 mg). The cooling curve was obtained from 20 to −90 °C and the heating curve from −90 to 400 °C with a rate of 5 °C/min.

Table 1 Chemical composition of the NIST B100 biodiesels produced from soy oil (SRM 2772) and animal feedstocks (SRM 2773)

Fatty chain	SRM 2772/wt%	SRM 2773/wt%
Lauric (C12:0)	–	0.05
Myristic (C14:0)	0.08	0.92
Pentadecanoic (C15:0)	–	0.03
Palmitic (C16:0)	10.70	18.40
Palmitoleic (C16:1)	0.13	2.33
Stearic (C18:0)	4.30	8.78
Oleic (C18:1)	23.30	34.30
Vaccenic (C18:1)	1.43	1.94
Linoleic (C18:2)	52.30	26.60
Linolenic (C18:3)	7.82	2.50
Arachidic (C20:0)	0.37	0.23
Arachidonic (C20:4)	–	0.25
Behenic (C22:0)	–	0.17

TG/derivative curves and infrared spectra were obtained on a TGA/DSC 1 Mettler-Toledo coupled to a FTIR Nicolet 6700 Thermo Scientific. Samples of about 10 mg were loaded in Al_2O_3 crucibles and measured in the temperature range from 25 to 400 °C with a heating rate of 5 °C/min under dynamic N_2 and synthetic air atmospheres (50 mL/min). Infrared spectra with spatial resolution of 4 cm^{-1} were collected periodically during the entire run.

Results and discussion

Cooling and heating DSC curves of SRM 2772 and SRM 2773 obtained with heating/cooling rate of 0.5 °C/min between 20 and −90 °C under inert atmosphere (N_2, 50 mL/min) are shown in Fig. 2. This heating/cooling rate allowed a very good separation of the events, mainly in cooling direction. Although endothermic transitions peaks observed along the heating curve indicate complete fusion of the esters in both biofuels initially solidified, the observed MPs related peaks are broadened, this behavior is consistent with mixtures of unsaturated and saturated long chain methyl esters [15]. Despite MPs onset temperatures are quite similar to those of T_{Cs}, the beginning of crystallization process during the cooling ramp is better defined and therefore, T_C was chosen as comparison parameter.

T_C for pure esters was determined by the same approach; the results are shown in Fig. 3. Saturated esters tend to crystallize above 0 °C (Fig. 3a), except methyl laurate which crystallizes at −3.5 °C. Differently of unsaturated esters (Fig. 3b), saturated esters crystallize in a highly exothermic process causing an increase in the temperature.

The peaks observed between 5 and −10 °C in Fig. 2 correspond to saturated esters crystallization present in

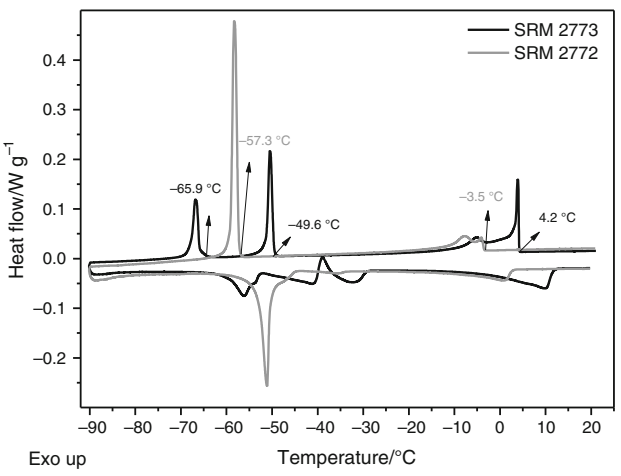

Fig. 2 Cooling (20 to −90 °C) and heating (−90 to 20 °C) DSC curves of SRM 2772 (*gray line*) and SRM 2773 (*black line*) samples under dynamic N_2 atmosphere (rate of 0.5 °C/min)

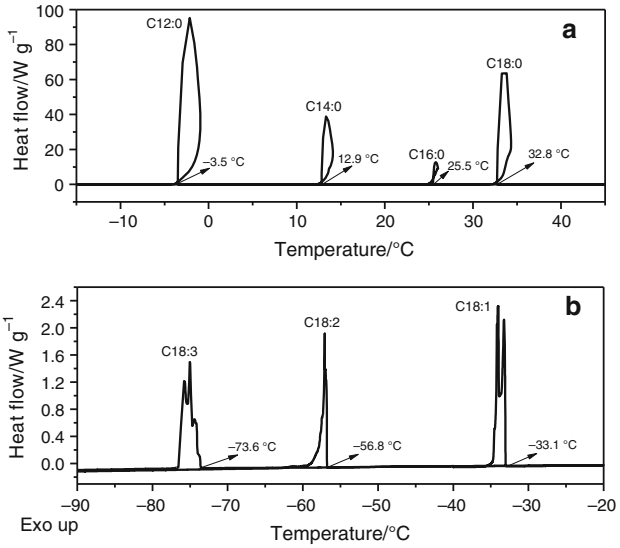

Fig. 3 Cooling (40 to −90 °C) DSC curves of pure esters samples under dynamic N_2 atmosphere (rate of 0.5 °C/min): **a** methyl laurate (C12:0), methyl myristate (C14:0), methyl palmitate (C16:0), methyl stearate (C18:0); **b** methyl oleate (C18:1), methyl linoleate (C18:2), methyl linolenate (C18:3)

both biodiesels. As the concentration of those esters in SRM 2773 is higher than in SRM 2772, representing 27.18 wt% against 15.45 wt% of the total composition, its T_C is also higher regarding the concentration of methyl palmitate and methyl stearate, about two times higher. Moreover, the T_C observed for each sample is pronouncedly below of that observed for pure saturated esters (Fig. 3a), indicating that the presence of unsaturated esters in higher amounts ends up to conduce the crystallization process. Furthermore, it is possible the occurrence of freezing-point depression phenomenon of each pure component present in the mixture, mainly for saturated esters [11].

For SRM 2772 an intense and single peak of crystallization in ca. −57.3 °C was observed (Fig. 2), this peak corresponds mainly to methyl linoleate T_C (−56.8 °C, Fig. 3b). This result shows that all the unsaturated esters crystallize together, prevailing the methyl ester T_C present in higher content (52.3 wt%). The proportions methyl linoleate/methyl oleate and methyl linoleate/methyl linolenate are 2.24:1 and 6.69:1, respectively, which explains the predominance of methyl linoleate over the others unsaturated esters and therefore the T_C value found.

For SRM 2773 two crystallization peaks were observed at low temperatures (Fig. 2): the first one starts at ca. −49.6 °C and the second one at ca. −65.9 °C. This analysis indicates that the first peak can be related to the crystallization of methyl oleate (−33.1 °C, Fig. 3b) and the second one to that of methyl linoleate (−56.8 °C, Fig. 3b), which are the main unsaturated esters present in this

biofuel, 34.3 and 22.6 wt%, respectively. The T_C depression can be attributed to the presence of other unsaturated long chain esters such as methyl linolenate (2.5 wt%) with T_C of −73.6 °C.

These results suggest that a freezing-point depression phenomenon occurs in both biodiesels in comparison to pure esters, likely due the presence of unsaturated esters which in turn can interact with each other and therefore these mixtures do not behave like ideal solutions as previously observed by Dunn [11]. Another feature must be taken into account: the esters ratio also influences the observed T_{Cs} in biodiesels.

The DSC curves shown in Fig. 4 were obtained cooling and heating the samples at rate of 5 °C/min between −90 and 450 °C in order to compare DSC and TG results. For both samples, the results at low temperatures are quite similar to those previously observed, with a slight shift of T_C and the absence of the small exothermic event occurring at ca. −40 °C in SRM 2773 biodiesel (Fig. 2), therefore, this event is related to the heating rate and has a kinetic nature and can be related to a re-organization process. Moreover, in the higher temperature range a large endothermic peak was observed beginning at about 170 °C for SRM 2773 biodiesel and about 180 °C for SRM 2772 biodiesel. This peak may be associated with the volatilization process of the different esters present into biodiesels in a single event. Thus, we can only infer that the lowest temperature observed for SRM 2773 is due to the presence of small chain esters (C12, C14, and C15) in higher amounts when compared with SRM 2772, whereas in its composition is almost twelve times lower.

TG was used to evaluate the two biodiesels thermal behavior under inert and oxidant atmospheres. Figure 5 shows TG/DTG curves of these biodiesels, for both

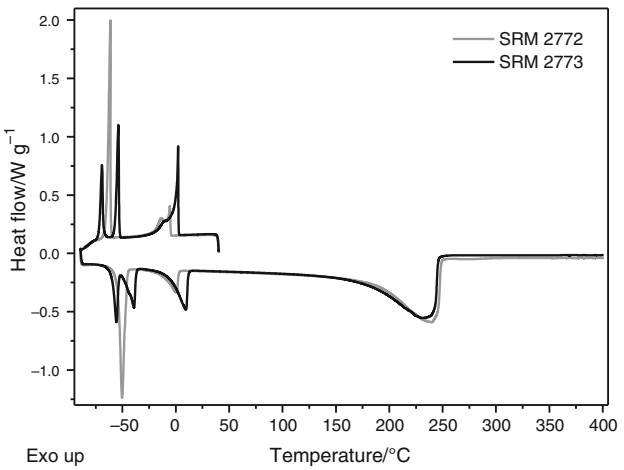

Fig. 4 Cooling (20 to −90 °C) and heating (−90 to 400 °C) DSC curves of SRM 2772 (*gray line*) and SRM 2773 (*black line*) samples under dynamic N_2 atmosphere (rate of 5 °C/min)

materials up to 100 °C, regardless the atmosphere used, there is no observable mass loss or gain and therefore, both of them are thermally stable in temperatures below this value. Also, both samples present only one thermal event with small onset temperature (T_{onset}) variations between each other due to the differences found in their composition (Table 1) [13, 14].

Differences between TG curves of these biodiesels under N_2 and synthetic air atmospheres are more pronounced in SRM 2772 sample (Fig. 5). For SRM 2772, the presence of higher amounts of unsaturated esters with more than one unsaturation in its composition shifts down the temperature values under synthetic air atmosphere, this trend can be explained by the low heat resistance and high susceptibility to oxidation when unsaturated esters are under an oxidizing atmosphere [16]. Furthermore, for SRM 2773, the beginning of mass loss occurs at lower temperature than for SRM 2772 under N_2 atmosphere as stated before from DSC curves analysis (Fig. 4). This observation just corroborates the previous results, which means that methyl esters with shorter chains and therefore lower boiling points will volatilize before than methyl esters with longer chains.

Besides the atmospheres do not modify the number of thermal events observed from DTG curves, they influence in residual mass as showed in Table 2. Decomposition residues are present in higher amounts in the end of analysis of SRM 2772 sample under oxidant atmosphere. It can be possible if one considers the presence of unsaturated esters with more than one unsaturation (60.12 wt%) in higher concentration than in SRM 2773 (29.35 wt%). These unsaturations can provide sites for oxidation by oxygen present in the atmosphere as well as molecule autoxidation can occur easily [16–18].

Infrared 3D diagrams collected during TG runs for the two biodiesels, SRM 2772 and SRM 2773 under synthetic air atmosphere, are presented in Fig. 6. They show the absorbance corresponding to the vibrational modes of the different chemical bonds and functional groups belonging to the molecules in the gases evolved from TG furnace while the temperature was raised at a rate of 5 °C/min versus the wavenumber and versus time. The absorbance maxima of each different vibrational modes in its characteristic wavenumber can be obtained crossing the diagram in a perpendicular way to the wavenumber axis, while examining the diagram in a perpendicular way to the time axis, the type of chemical bonds present in the these gases at each time/temperature can be obtained [19].

Despite the analysis of 3D diagrams provide useful information about the temporal evolution of the reactions under study the interpretation of such spectra is quite difficult because the complexity of the samples which

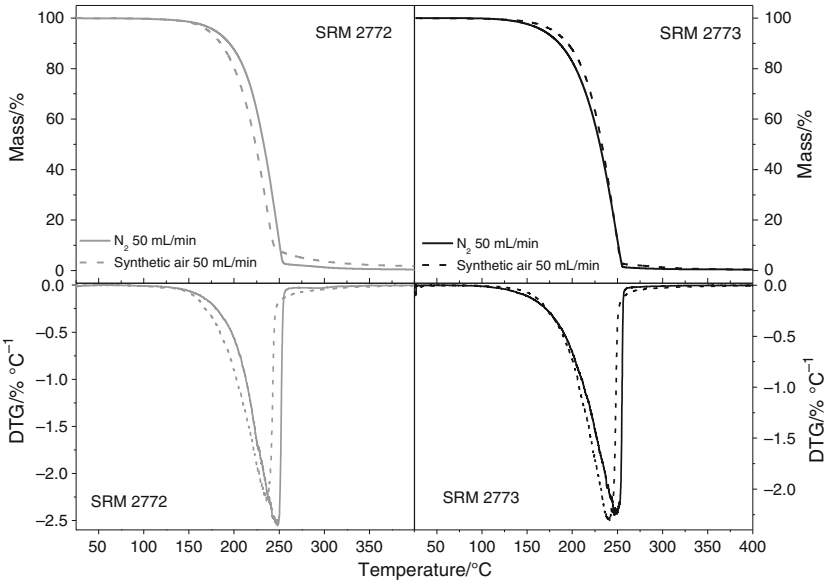

Fig. 5 TG/DTG curves of SRM 2772 (*gray lines*) and SRM 2773 (*black lines*) under dynamic atmospheres of N_2 and synthetic air (50 mL/min). Heating rate of 5 °C/min

Table 2 Mass loss determined from TG curves of both samples under N_2 and synthetic air atmospheres

	N_2		Synthetic air	
	Δm_1/%	Δm_2/%	Δm_1/%	Δm_2/%
SRM 2772	97.6	1.9	93.1	5.5
SRM 2773	98.6	0.9	95.8	3.3

originates a complex mixture of volatilized compounds. The FTIR spectra can correspond to the absorption of those compounds obtained during the maximum decomposition rates and also to tails from those compounds associated to different decomposition processes [19].

Establishing a relationship between TG/DTG curves (Fig. 5) and the 3D diagram of Fig. 6a, the maxima of volatilized products generation can be found. These maxima are coincident with the maxima of absorbance observed in the scale of relative time of 5, 20, and 40 min (first step at around 25, 100, and 200 °C, respectively), and 70 min (second step, at around 350 °C).

The FTIR spectra showed in Fig. 7 correspond to the temperatures cited above and the absorption bands observed are related to characteristic bonds of unsaturated esters, which are the major constituents of biodiesels, and of some products that can be formed during oxidation reaction. C=O stretching absorption is characteristic of the IR spectra of carbonylic compounds, in the case of esters, this band appears in the 1750–1735 cm^{-1} region. A strong band corresponding to ethers C–O–C bond appears in the 1200–900 cm^{-1} region [20–22], this kind of bond can be formed by processes such as radical recombination [16]. The absorption bands characteristic of C–H bonds appear in 3019 cm^{-1} corresponding to the stretching vibrational

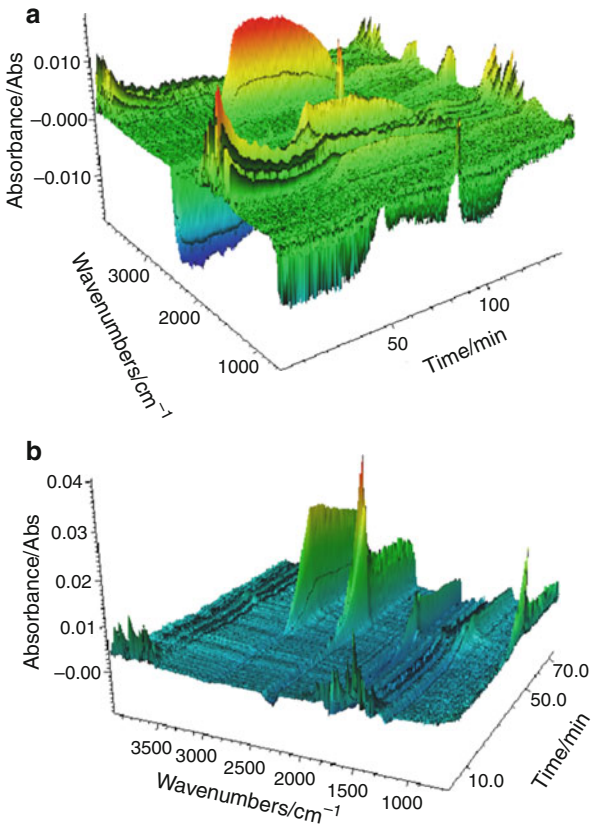

Fig. 6 3D IR spectra of **a** SRM 2772 and **b** SRM 2773 under oxidizing dynamic atmosphere (synthetic air, 50 mL/min and heating rate of 5 °C/min)

mode of alkenes C=C–H, in 3019 and 2962 cm^{-1} corresponding to the asymmetric and symmetric vibrational modes of methyl groups, respectively, and in 2933 and 2864 cm^{-1} corresponding to the asymmetric and

symmetric vibrational modes of methylene groups, respectively [19].

The absorption bands of OH bond (Fig. 7) can be observed due probably of glycerol presence, since it is a byproduct of transesterification reaction and is present in higher amounts in SRM 2772 than in SRM 2773, 164 and 12.1 mg/kg, respectively [13, 14]. Also water can contribute to absorption above 3500 cm^{-1}; however, it seems that more vibrational modes contribute to the bands in the range of 1650–1200 cm^{-1} [19]. On the other hand, downward peaks, occurring in the range of 2460–2190 cm^{-1}, correspond to the decrease in CO_2 concentration (due to a poor purge) in the systems.

Similar analysis was carried out for the SRM 2773 that corresponds to animal feedstocks biodiesel. In this case, the same line shape for all spectra and the formation of greater amounts of CO_2 than for the SRM 2772 can be observed. These results strongly suggest that SRM 2773 underwent partial combustion in a higher degree than the other biodiesel sample and therefore explain the lesser amount of residual mass observed at the end of the experiment.

According to mechanisms proposed previously despite C–C bonds are weaker than C–O or O–C=O bonds, the cleavage of the carbon chain is difficult to occur being necessary some special activation to promote the formation of aldehydes. The activation process begins with the reaction between the methyl ester molecules with O_2, the mechanism involves radical species formation and then their combination with O_2 molecules to form peroxides. In unsaturated esters the double bonds are broken only in the final oxidation steps [18, 19, 23, 24].

Both biodiesels did not undergo complete combustion, however, some evidences of chains oxidation can be obtained from FTIR spectra (Figs. 7, 8). Although peroxide formation is very difficult to observe in FTIR spectra because its signal intensity is very weak and from the interference of carbon skeletal modes in the range 845–875 cm^{-1} [25, 26], at temperatures lower than 300 °C, the intensity of the band corresponding to C=C bond at ca. 3019 cm^{-1} is very small mainly in SRM 2773. Also, the formation of ethers from radical combination at temperatures above 200 °C was identified.

Two other points deserve some attention concerning the oxidation mechanism, the first one is related to the other stretching modes, if the oxidation stopped in the peroxide formation and cleavage of C=C bonds, the vibrational modes corresponding to the ester groups still will be detectable (Fig. 7); the second point comes from the oxidation kinetics, some fragments of dienes from C–C bond cleavage can be formed at temperatures above 250 °C. These fragments will depend on the number and position of the C=C bonds [2, 17], this feature is more pronounced in SRM 2772 where methyl linoleate is its major constituent: 52.30 wt%.

The FTIR results from experiments performed under N_2 atmosphere presented absorption bands with lower intensities, this feature can be explained by the lack of optimization of the relation between heating rate and carrier gas flow which in turn will determine the kind of instrument response [27]. Also, there is a relation between this parameter and the kind of gas used in the experiment, in

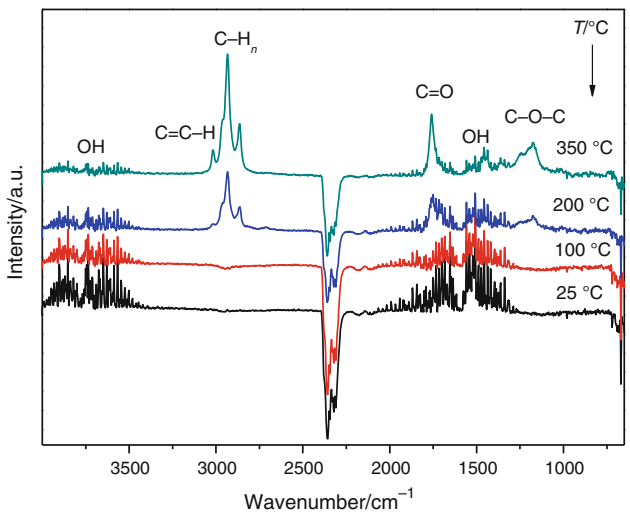

Fig. 7 IR spectra of SRM 2772 sample under synthetic air atmosphere at different temperatures (heating rate of 5 °C/min and flux of 50 mL/min)

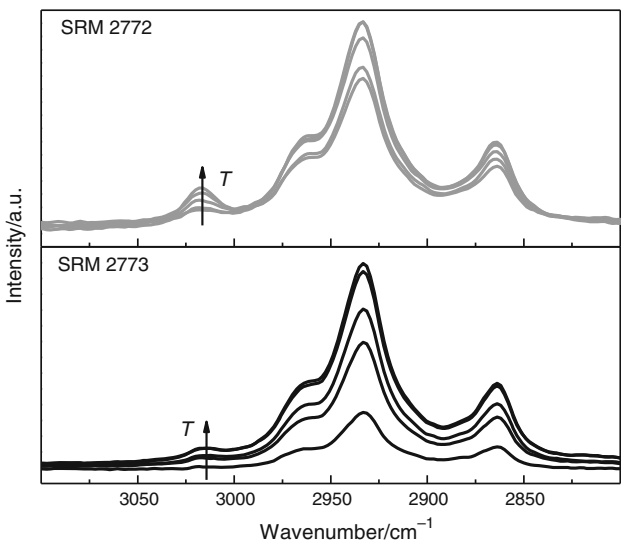

Fig. 8 Expanded portion of IR spectra of SRM 2772 (*gray lines*) and SRM 2773 (*black lines*) samples under dynamic synthetic air atmosphere at different temperatures (heating rate of 5 °C/min and flux of 50 mL/min)

consequence a relation which works with one kind of gas maybe is not appropriate to another.

Basically, the absorption trends observed for both samples are almost the same of those observed in experiments under synthetic air, exception that the cleavage of C=C bonds were not detected in SRM 2773. In these experimental situations is reasonable to believe that almost all the compounds volatilized since no char products was observed, the main residual products expected are polymers from unsaturated ester polymerization.

Conclusions

By applying TA techniques for biofuels thermal behavior characterization some advantages and disadvantages were found. As advantages we can point to DSC studies of MP and T_C in temperature range 20 to −90 °C. The results showed that is possible the comparison between pure esters T_{Cs} with those found in DSC biodiesels curves, aiming their main composition and therefore predict each biodiesel application in different places with different weather, and the need for additives use to prevent their freezing in tanks and pipes. Moreover, as disadvantages the DSC curves analysis in high temperatures (above 100 °C), was more complicated. Thermal events could not be separated, therefore is difficult to conclude anything based only in esters boiling points, for example, and there is no evidence of decomposition processes.

Together with TG/FTIR data, some remarks can be done. These studies also tested biodiesels thermal behavior under synthetic air atmosphere. Up to 100 °C regardless the atmosphere used during the analysis, both biodiesels do not present any mass gain or loss; therefore they are thermally stable below this temperature. Above that they present one thermal event with small differences in temperatures between samples due to differences in the percentage of esters in their chemical composition.

Although the coupled techniques TG/FTIR are useful for differentiating biodiesels of different compositions, these alone do not provide indications about the mechanism of thermal decomposition of such complexes matrices. In order to provide a better understanding of mechanistic aspects the use of a technique that unambiguously indicate the products formed, such as mass spectrometry or chromatography, is necessary.

Acknowledgements The authors are grateful to the Brazilian agencies: Financiadora de Estudos e Projetos (FINEP), Fundação de Amparo à Pesquisa do Estado do Rio de Janeiro (FAPERJ), and Conselho Nacional de Desenvolvimento Científico e Tecnológico (CNPq).

References

1. Meher LC, Vidya Sagar D, Naik SN. Technical aspects of biodiesel production by transesterification—a review. Renew Sustain Energy Rev. 2006;10:248–68.
2. USEPA. A comprehensive analysis of biodiesel impacts on exhaust emissions (Draft technical report No. EPA420-P-02-001). Washington, DC: US Environmental Protection Agency; 2002.
3. Conceição MM, Fernandes VJ, Bezerra AF, Silva MCD, Santos IMG, Silva FC, Souza AG. Dynamic kinetic calculation of castor oil biodiesel. J Therm Anal Calorim. 2007;87:865–9.
4. Xiaoxiang J, Ellis N, Zhaoping Z. Fuel properties of bio-oil/biodiesel mixture characterized by TG, FTIR and ^{1}H NMR. Korean J Chem Eng. 2011;28:133–7.
5. Chien Y-C, Lu M, Chai M, Boreo FJ. Characterization of biodiesel, biodiesel particulate matter by TG, TG-MS and FTIR. Energy Fuels. 2009;23:202–6.
6. Chand P, Reddy Ch V, Verkade JG, Wang T, Grewell D. Thermogravimetric quantification of biodiesel produced via alkali catalyzed transesterification of soybean oil. Energy Fuels. 2009;23:989–92.
7. Rodriguez RP, Sierens R, Verhelst S. Thermal and kinetic evaluation of biodiesel derived from soybean oil and higuereta oil. J Therm Anal Calorim. 2009;96:897–901.
8. Freire LMS, Bicudo TC, Rosehaim R, Sinfrônio FSM, Botelho JR, Carvalho Filho JR, Santos IMG, Jr Fernandes VJ, Antoniosi Filho NR, Souza AG. Thermal investigation of oil and biodiesel from *Jatropha curcas* L. J Therm Anal Calorim. 2009;96:1029–33.
9. Santos NA, Santos JRJ, Sinfrônio FSM, Bicudo TC, Santos IMG, Antoniosi Filho NR, Fernandes VJ Jr, Souza AG. Thermo-oxidative stability and cold flow properties of babassu biodiesel by PDSC and TMDSC techniques. J Therm Anal Calorim. 2009;97(2):611–4.
10. Dunn RO. Thermal analysis of alternative diesel fuels from vegetable oils. J Am Oil Chem Soc. 1999;76(1):109–15.
11. Dunn RO. Crystallization behavior of fatty acid methyl esters. J Am Oil Chem Soc. 2008;85:961–72.
12. Jain S, Sharma MP. Thermal stability of biodiesel and its blends: a review. Renew Sustain Energy Rev. 2011;15:438–48.
13. Standard Reference Material 2772. B100 biodiesel (soy-based). In: National Institute of Standards and Technology, 2009. https://www-s.nist.gov/srmors/view_detail.cfm?srm=2772.
14. Standard Reference Material 2773. B100 biodiesel (animal-based). In: National Institute of Standards and Technology, 2009. https://www-s.nist.gov/srmors/view_detail.cfm?srm=2773.
15. Knothe G, Dunn RO. A comprehensive evaluation of the melting points of fatty acids and esters determined by differential scanning calorimetry. J Am Oil Chem Soc. 2009;86:843–56.
16. Pillar R, Ginic-Markovic M, Clarke S, Matisons J. Effect of alkyl chain unsaturation on methyl ester thermo-oxidative decomposition and residue formation. J Am Oil Chem Soc. 2009;86:363–73.
17. Dantas MB, Albuquerque AR, Barros AK, Rodrigues Filho MG, Antoniosi Filho NR, Sinfrônio FSM, Rosenhaim R, Soledade LEB, Santos IMG, Souza AG. Evaluation of the oxidative stability of corn biodiesel. Fuel. 2011;90:773–8.
18. Schneider C, Porter NA, Brash AR. Routes to 4-hydroxynonenal: fundamental issues in the mechanism of lipid peroxidation. J Biol Chem. 2008;283:15539–43.
19. Marcilla A, Gómez-Siurana A, Gomis C, Chápuli E, Catalá MC, Valdés FJ. Characterization of microalgal species through TGA/FTIR analysis: application to *nannochloropsis* sp. Thermochim Acta. 2009;484:41–7.

20. Yan R, Yang H, Chin T, Liang DT, Chen H, Zheng C. Influence of temperature on the distribution of gaseous products from pyrolyzing palm oil wastes. Combust Flame. 2005;142(1–2): 24–32.
21. Yang H, Yan R, Chen H, Lee DH, Zheng C. Characteristics of hemicellulose, cellulose and lignin pyrolysis. Fuel. 2007;86: 1781–8.
22. Kansiz M, Heraud P, Wood B, Burden F, Beardall J, McNaughton D. Fourier transform infrared microspectroscopy and chemometrics as a tool for the discrimination of cyanobacterial strains. Phytochemistry. 1999;52:407–17.
23. Herbinet O, Pitz WJ, Westbrook CK. Detailed chemical kinetic oxidation mechanism for a biodiesel surrogate. Combust Flame. 2008;154:507–28.
24. Wetbrook CK, Naik CV, Herbinet O, Pitz WJ, Mehl M, Sarathy SM, Curran HJ. Detailed chemical kinetic reaction mechanisms for soy and rapeseed biodiesel fuels. Combust Flame. 2011;158: 742–55.
25. Shreve OD, Heether MR, Knight HB, Swern D. Infrared absorption spectra of some hydroperoxides, peroxides, and related compounds. Anal Chem. 1951;23:282–5.
26. Vacque V, Sombret B, Huvenne JP, Legrand P, Suc S. Characterization of the O–O peroxide bond by vibrational spectroscopy. Spectrochim Acta A. 1997;53:55–66.
27. Berbenni V, Marini A, Bruni G, Zerlia T. TG/FT-IR: an analysis of the conditions affecting the combined TG/spectral response. Thermochim Acta. 1995;258:125–33.